

# Origin and annealing of deep-level defects in *p*-type GaAs/Ga(As,N)/GaAs heterostructures grown by molecular beam epitaxy

P. Krispin<sup>a)</sup>

*Paul-Drude-Institut für Festkörperelektronik, Hausvogteiplatz 5-7, 10117 Berlin, Germany*

S. G. Spruytte and J. S. Harris

*Solid State and Photonics Laboratory, Stanford University, Stanford, California 94305*

K. H. Ploog

*Paul-Drude-Institut für Festkörperelektronik, Hausvogteiplatz 5-7, 10117 Berlin, Germany*

(Received 8 November 2000; accepted for publication 12 March 2001)

Deep-level defects in *p*-type GaAs/Ga(As,N)/GaAs heterostructures grown by molecular beam epitaxy are investigated by deep-level transient Fourier spectroscopy. Depth-resolved distributions of hole traps are measured in as-grown and annealed heterojunctions in order to identify the defects, which lead to the degradation of the Ga(As,N) properties. Four defects are recognized in the heterostructures studied. Two dominant hole traps are found in Ga(As,N) at energies of about 0.35 and 0.45 eV above the valence band edge. These midgap levels originate from copper- and iron-related defects, the formation of which is connected with operation of the nitrogen plasma cell during Ga(As,N) growth. Both traps, which are removed by annealing, are discussed as the possible nonradiative centers that deteriorate the optical properties. Two other hole traps of intrinsic origin are related to the GaAs growth conditions close to the Ga(As,N)-on-GaAs interface, where the GaAs growth is affected by the nitrogen plasma despite a closed shutter. As far as electronic levels in the lower half of the band gap are concerned, the Ga(As,N) layers and GaAs-on-Ga(As,N) interfaces become practically defect free after rapid thermal annealing. © 2001 American Institute of Physics. [DOI: 10.1063/1.1370115]

## I. INTRODUCTION

The introduction of small amounts of nitrogen into GaAs leads to unique optical properties, because the band gap decreases drastically with increasing GaN composition.<sup>1,2</sup> Recently, we have experimentally shown that GaAs/Ga(As,N) heterointerfaces are of type I.<sup>3</sup> For a band gap difference  $\Delta E_G$  of about 430 meV, a comparatively small valence band offset  $\Delta E_V$  of 11 meV has been found, as expected from the large electronegativity of nitrogen.<sup>3</sup> The (Ga,In)(As,N) materials system has attracted considerable attention for a wide range of potential applications in optoelectronic devices,<sup>4-7</sup> particularly, in vertical-cavity surface-emitting laser diodes<sup>8-10</sup> and solar cells.<sup>11</sup> Unfortunately, the crystal quality has been found to deteriorate for higher concentrations of incorporated nitrogen, leading to a strong degradation of the optical properties.<sup>12-14</sup> It has been further established that there is a distinct carrier depletion in as-grown Ga(As,N) layers embedded in GaAs.<sup>3</sup> It is not clear yet whether the material degradation is due to phase separation,<sup>15,16</sup> displaced nitrogen atoms in the Ga(As,N) lattice,<sup>17</sup> impurities from the N source,<sup>13</sup> or intrinsic defects formed during growth under tensile strain.

The crystal quality and the luminescence efficiency of Ga(As,N) layers can be remarkably improved by postgrowth annealing.<sup>12-14,17</sup> The carrier deficit in *p*-type GaAs/

Ga(As,N)/GaAs heterostructures can also be removed by rapid thermal annealing (RTA),<sup>3</sup> i.e., the concentration of lattice imperfections in the as-grown Ga(As,N) layer can be strongly reduced. In particular, donor-like defects have been verified to be responsible for the carrier depletion in Ga(As,N).<sup>3</sup>

Because the defects, which give rise to the degradation of Ga(As,N) properties, have not been identified up to now, *p*-type GaAs/Ga(As,N)/GaAs heterostructures grown by molecular beam epitaxy (MBE) have been examined by capacitance versus voltage (*C-V*) measurements<sup>18</sup> and deep-level transient Fourier spectroscopy (DLTFS).<sup>19</sup> In order to investigate the Ga(As,N) layers and also the normal [Ga(As,N)-on-GaAs] and inverted [GaAs-on-Ga(As,N)] interfaces, depth-resolved distributions of deep-level defects have been measured in as-grown and annealed isotype heterojunctions.

Two dominant hole traps are found in Ga(As,N) at energies of about 0.35 and 0.45 eV above the valence band edge  $E_V$ . Both midgap levels originate from impurity-related defects, which are formed during Ga(As,N) growth. The two traps, which can be removed by annealing, are discussed as the possible sources of the degradation of the electronic properties of Ga(As,N). After rapid thermal annealing, the Ga(As,N) layers and GaAs-on-Ga(As,N) interfaces are practically defect free as far as traps in the lower half of the Ga(As,N) band gap are concerned.

<sup>a)</sup>Electronic mail: krispin@pdi-berlin.de

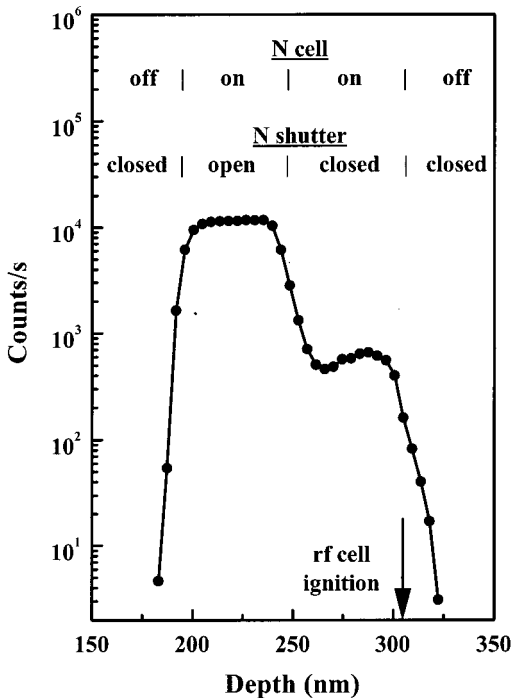


FIG. 1. Typical depth profile of nitrogen measured by SIMS for as-grown sample No. 1. The rf plasma ignition point is indicated by the arrow. The operation of the N cell and the position of the N shutter are sketched for the different regions.

**II. EXPERIMENTAL DETAILS**

**A. Samples**

The GaAs/Ga(As,N)/GaAs heterostructures investigated were grown by elemental source MBE on  $p^+$ -type GaAs(001) substrates. Dimeric arsenic and atomic nitrogen were provided by a thermal cracker and a radio frequency (rf) nitrogen plasma cell, respectively. Details of the growth are published elsewhere.<sup>17</sup> The layer structure consisted of about 1  $\mu\text{m}$  Be-doped GaAs grown at 620 °C, the Ga(As,N) layer grown at 500 °C, and approximately 200 nm Be-doped GaAs grown at 620 °C on top. Changes in the growth temperature took 2 min and were performed during GaAs growth. The GaAs regions grown during this gradual temperature change were about 15 nm thick. The GaN mole fraction of the Ga(As,N) layer was 3% as determined from high resolution x-ray diffraction (HRXRD) measurements and calibrated secondary ion mass spectrometry (SIMS). We observed no strain relaxation which was checked by HRXRD. In this article, two samples with unintentionally (No. 1) and Be-doped (No. 2) Ga(As,N) were investigated.

RTA was performed *ex situ* for 60 s at 760 °C under  $\text{N}_2$  atmosphere using a GaAs wafer in close proximity to the investigated heterostructures. It is known that the photoluminescence intensity of Ga(As,N) can be strongly enhanced under these annealing conditions.<sup>14,17</sup>

For the layer sequence with unintentionally doped Ga(As,N) (sample No. 1), a typical SIMS depth profile of the nitrogen concentration is plotted in Fig. 1. The two interfaces between GaAs and Ga(As,N) at about 200 and 250 nm are well defined. The strong change in the N concentration at

about 305 nm is associated with the ignition of the rf plasma and shows that a certain N flux bypasses the closed shutter of the N cells. The GaN mole fraction in the 50 nm thick GaAs layer grown before Ga(As,N) is estimated to be less than 0.2%. The metal–semiconductor (MS) contacts for the electrical measurements were formed by vacuum-deposited Ti/Au dots on the GaAs top layer. Ohmic contacts were realized with Au/Be on the  $p^+$ -type GaAs substrate.

**B. C–V method**

Capacitance and ac conductance were measured with a HP admittance meter (4275A). The loss factor was kept below 0.1. The depth profile of the apparent hole concentration  $N_{C-V}$  was measured using the conventional C–V method.<sup>18</sup> The concentration  $N_{C-V}$  was obtained from the expression

$$N_{C-V}(W) = \frac{2}{A^2 q \epsilon \epsilon_0} \left[ \frac{d}{dV} \left( \frac{1}{C^2} \right) \right]^{-1}, \tag{1}$$

where  $W$  denotes the thickness of the space-charge layer below the MS contact,  $A$  the contact area,  $q$  the elementary charge, and  $\epsilon \epsilon_0$  the dielectric constant. In general,  $N_{C-V}$  is equal to the free hole density  $p$  at the edge of the space charge layer.<sup>18</sup> The depth  $W$  was calculated from the depletion capacitance  $C$  using  $W(V) = \epsilon \epsilon_0 A / C(V)$ . By changing a dc bias in the reverse direction, the edge of the space-charge layer below the contact could be shifted across the Ga(As,N) layer. The hole concentration of GaAs measured by the C–V method was about  $3 \times 10^{16} \text{ cm}^{-3}$ . The hole density in the Ga(As,N) layers was obtained from the C–V depth profiles by simulations based on self-consistent solutions of the Poisson equation (see Ref. 3).

For nondegenerate semiconductor structures, the spatial resolution of the carrier density versus depth profile is limited by the Debye screening length  $L_D = \sqrt{\epsilon \epsilon_0 k T / p q^2}$ , where  $k$  denotes the Boltzmann constant and  $T$  the temperature. For a hole density  $p$  of  $3 \times 10^{16} \text{ cm}^{-3}$ , the  $L_D$  values are about 13 and 25 nm at 80 and 300 K, respectively.

**C. Deep-level transient Fourier spectroscopy**

Deep-level spectra were measured with a computer-controlled BioRad DLTFs system (DL8000). In temperature scans, the capacitance–time transients were digitized, and the discrete Fourier coefficients were calculated at each temperature by numerical Fourier transformation.<sup>19</sup> For this article, temperature scans of the first sine coefficient  $b_1$  were evaluated. The effective thermal activation energy  $E_{th}$  of hole traps was obtained from the temperature dependence of the emission rate  $e_p$  for holes from the level into the valence band<sup>20</sup>

$$e_p = \sigma_p v_{th} N_V \exp\left(-\frac{E_{th}}{kT}\right), \tag{2}$$

where  $\sigma_p$  denotes the capture cross section of the deep level for holes at high temperature,  $v_{th}$  the thermal velocity of holes in the valence band, and  $N_V$  the effective density of states of the valence band. The emission rate  $e_p$  was found by analyzing the peak positions in temperature scans for different Fourier coefficients. Deep levels were identified by

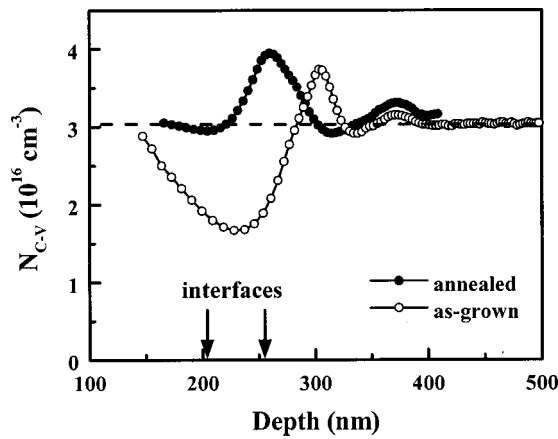


FIG. 2. Typical depth profiles of the apparent hole concentration  $N_{C-V}$  for as-grown and annealed GaAs/Ga(As,N)/GaAs structures. The plots were measured at 300 K and 1 MHz for the GaAs/Ga(As,N)/GaAs structure with undoped Ga(As,N) (sample No. 1). The dashed line indicates constant doping level of  $3 \times 10^{16} \text{ cm}^{-3}$  in the entire heterostructure. The positions of the two heterointerfaces are marked by arrows.

plotting  $\log(e_p/T^{-2})$  vs  $1/T$ . On the basis of these Arrhenius plots, a comparison was made with published data. Note that the energy  $E_{th}$  is the sum of the true deep-level energy  $E_t$  and the activation energy  $E_\sigma$  for the capture process if the capture process is also thermally activated.

The deep-level concentration  $N_t$  was determined from the DLTFs peak height  $\Delta C_m/C$  according to the full correction given in Ref. 21:

$$\frac{\Delta C_m}{C} = \frac{N_t}{2p} \frac{(W_R - \lambda)^2 - (W_P - \lambda)^2}{W_R^2}, \quad (3)$$

where  $W_R$  and  $W_P$  denote the thicknesses of the depletion layer at the quiescent reverse bias and at the pulse voltage, respectively, and

$$\lambda = \sqrt{\frac{2\epsilon\epsilon_0(E_F - E_t)}{q^2 p}}. \quad (4)$$

The point  $(W - \lambda)$  below the MS contact indicates the position where the Fermi level  $E_V + E_F$  crosses the deep level  $E_V + E_t$ . The deep-level response therefore originates from a depth around  $[(W_R + W_P)/2 - \lambda]$ . In order to fully evaluate corrected concentration versus depth profiles for a certain hole trap,  $W_R$ ,  $W_P$ , and  $\lambda$  were determined at the temperature of the related DLTFs peak.

### III. RESULTS AND DISCUSSION

#### A. Depth profiles of the apparent carrier density

Typical depth profiles of the apparent hole density  $N_{C-V}$  are depicted in Fig. 2. For as-grown heterostructures, the carrier depletion in the Ga(As,N) layer and the two peaks above 300 nm are characteristic. A remarkably large number of donor-like defects apparently occurs in as-grown Ga(As,N). The nodes found at 310 and 370 nm are not related to real variations of the bulk hole density, but are due to capacitance contributions of interfacial deep states.<sup>3</sup> When the Fermi level crosses an interfacial level at sufficiently high reverse biases, captured holes are released and give rise

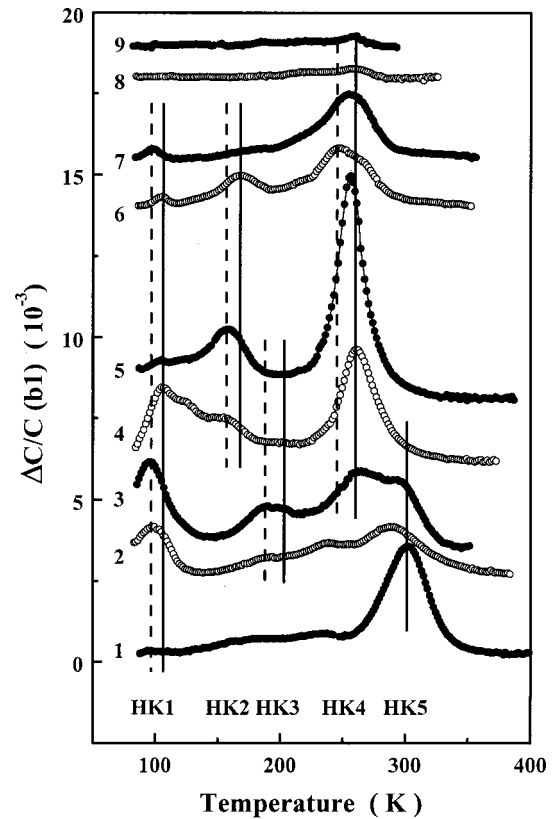


FIG. 3. Deep-level spectra (Fourier coefficient  $b_1$ , 100 ms pulse width, 1 s period) for as-grown GaAs/Ga(As,N)/GaAs structure No. 1. Spectra 1–9, which correspond to increasing quiescent biases, are vertically shifted for clarity. The pulse height was 0.5 V. For hole traps HK1–HK5 in Ga(As,N) and GaAs, the temperature positions of the DLTFs peaks are marked by dashed and solid lines, respectively.

to this remarkable carrier enhancement. That part of the depth profile can therefore be employed for a spectroscopy of interface traps (release spectroscopy). In particular, the two nodes in Fig. 2 are due to two levels at about  $E_V + 0.16$  and  $+0.32$  eV at the normal interface of GaAs/Ga(As,N)/GaAs structures.<sup>3</sup>

After annealing, the carrier deficit in the Ga(As,N) layer is completely removed. Free holes are found, which are mainly due to shallow dopants in the Ga(As,N) layer. Additional holes originate from both GaAs regions adjacent to the Ga(As,N) layer, which are weakly depleted. This transfer of holes from GaAs to the higher valence band edge of Ga(As,N) in conjunction with the smaller band gap of Ga(As,N) indicates the type-I character of GaAs/Ga(As,N) interfaces.<sup>3</sup> Because the Be concentration in unintentionally doped Ga(As,N) has been found by SIMS to be lower than  $5 \times 10^{14} \text{ cm}^{-3}$ , the hole density of  $3 \times 10^{16} \text{ cm}^{-3}$  for the annealed sample in Fig. 2 is due to other impurities (like carbon) or intrinsic shallow-level defects in the Ga(As,N) layer.

#### B. Deep-level spectra

For the as-grown GaAs/Ga(As,N)/GaAs structure No. 1 studied above, spectra of the first Fourier coefficient  $b_1$  are shown in Fig. 3 as relative capacitance changes  $\Delta C/C$  versus temperature under various bias conditions. The positive DLTFs signals are attributed to hole traps in  $p$ -type material.

TABLE I. Summary of results concerning the deep-level defects in as-grown *p*-type GaAs/Ga(As,N)/GaAs heterostructures. DLTFs peak temperature and thermal activation energy are provided for hole traps in GaAs as well as in Ga(As,N).

Deep level	DLTFs peak temperature <sup>a</sup> (K)		Thermal activation energy $E_{th}$ (eV)		Maximal Density close to	Removal by annealing
	Ga(As,N)	GaAs	Ga(As,N)	GaAs		
HK1	95	105	0.16	0.18	Normal interface	No
HK2	158	168	0.39	0.39	Normal interface	No
HK3	190	205	0.35	0.37	Inverted interface	Yes
HK4	250	260	0.55	0.55	Inverted interface	Yes
HK5	...	300	...	0.69	GaAs cap surface	Yes

<sup>a</sup>Measured at 1 s period.

For bulk levels, different bias conditions correspond to different depths. An interfacial trap can be observed only at a certain bias when the Fermi level crosses the electronic state at the interface.

The sample investigated exhibits a sequence of distinct peaks labeled HK1–HK5, which are found in all GaAs/Ga(As,N)/GaAs heterostructures. The associated DLTF responses emerge only under certain bias conditions. Level HK4 is dominant in as-grown sample No. 1. A striking property of the level responses concerns the shift of the respective peak temperatures. For example, the response of hole trap HK4 is observed in the lower bias range (curves 3 and 4) at 260 K. This peak shifts at intermediate bias values towards 250 K (curves 5 and 6) and then back to 260 K at sufficiently high reverse biases (curves 8 and 9). The shift is mainly due to a small change of the thermal activation energy  $E_{th}$ . Such behavior is characteristic for a distinct defect, the electronic level of which changes with composition. For level HK4, the DLTFs peaks at low, intermediate, and high reverse biases in Fig. 3 can be associated with the same defect in the upper GaAs, the Ga(As,N) and the bottom GaAs layers, respectively. The defects related to levels HK1–HK4 apparently occur in both materials of the heterostructure, but with strong spatial variations of the concentrations. On the contrary, level HK5 is found only at low reverse biases (see curves 1–3 in Fig. 3), i.e., exclusively at the GaAs surface of as-grown samples. It disappears completely after annealing.

The DLTFs results are compiled in Table I for all deep levels which have been detected in the MBE-grown *p*-type GaAs/Ga(As, N)/GaAs heterostructures.

**C. Depth profiles of deep-level concentrations**

**1. Hole trap HK1**

Typical concentration versus depth profiles for hole trap HK1 in as-grown and annealed GaAs/Ga(As, N)/GaAs structures are depicted in Figs. 4(a) and 4(b), respectively. The distribution of level HK1 is identical for all investigated heterostructures with different thicknesses or hole densities of the embedded Ga(As, N) layer. The depth profile does not change after annealing. The depth scales in Fig. 4 have been determined by using the thermal activation energy  $E_{th}$  instead of the level energy  $E_t$  (see Sec. II C and Table I). Hole trap HK1 is concentrated near the normal interface at 250 nm. The position of the normal interface measured by the

*C*–*V* method at 100 K is in accordance with the SIMS profile in Fig. 1, which was measured on the same sample No. 1. The depth scale in Fig. 4 is further confirmed by the shift of the DLTFs peak temperature from 95 (circles) to 105 K (dots) at the very position of the normal interface. The use of the thermal activation energy  $E_{th}$  instead of the true level energy  $E_t$  is apparently allowed for hole trap HK1, i.e., the hole capture process is not thermally activated.

The energy of level HK1 changes from 0.16 to 0.18 eV by crossing the interface from Ga(As, N) to GaAs. It is the same defect which gives rise to the two discrete levels on both sides of the heterojunction. Surprisingly, there is a further shift of the DLTFs peak temperature for trap HK1 from curve 6 to curve 7 in Fig. 3. The lower DLTFs peak temperature, which is characteristic for Ga(As, N), is found in the depth profile at about 310 nm [see the square symbol in Fig. 4(a)]. Within experimental accuracy, this position matches the ignition point of the rf plasma (cf. Fig. 1). Although the shutter of the N cell is still closed, the related defect is apparently formed in the bottom GaAs layer when

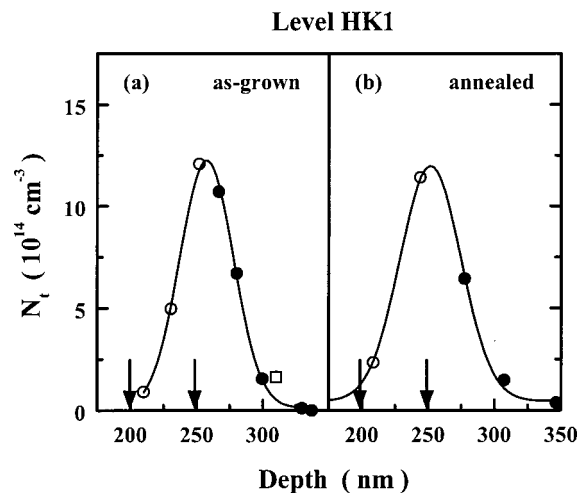


FIG. 4. Typical concentration vs depth profiles for hole trap HK1 derived from deep-level spectra on (a) the as-grown and (b) annealed heterostructure No. 1. The interface positions are indicated by arrows. The DLTFs peak temperatures of 95 and 98 K for Ga(As,N) and 105 K for GaAs are marked by circles, square, and dots, respectively. The data are fitted by Gaussian curves. The density of level HK1 at the normal interface is found to be about  $6 \times 10^9 \text{ cm}^{-2}$  for the as-grown and annealed samples.

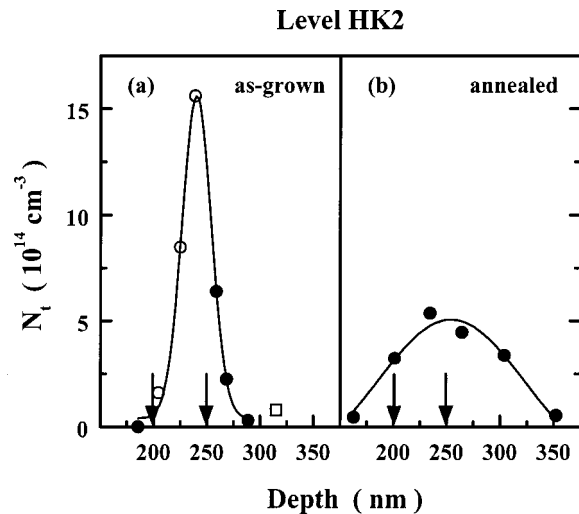


FIG. 5. Concentration vs depth profiles for hole trap HK2 derived from deep-level spectra on (a) the as-grown and (b) annealed heterostructure No. 1. The interface positions are indicated by arrows. The DLTFs peak temperatures of 158 and 160 K for Ga(As,N) and 168 K for GaAs are marked in (a) by circles, square, and dots, respectively. For the annealed sample in (b), the exact peak temperatures could not be determined due to the broad and weak response. The data are fitted by Gaussian curves. The density of level HK2 at the normal interface is found to be about  $6 \times 10^9 \text{ cm}^{-2}$  for the as-grown and annealed samples.

the plasma source is ignited. Defect HK1, however, does not seem to be linked with nitrogen itself, since the defect concentration decreases inside the Ga(As, N) layer during growth. The growth of *p*-type GaAs is apparently affected by the rf plasma.

It should be noted that level HK1 around  $E_V + 0.17 \text{ eV}$ , which is observed in this article by the DLTFs technique, has been also found by release spectroscopy.<sup>3</sup> Since peaks in release spectra originate solely from spatially confined electronic states, the predominant interfacial character of level HK1 is hereby confirmed.

## 2. Hole trap HK2

For as-grown and annealed sample No. 1, concentration versus depth profiles of level HK2 are shown in Figs. 5(a) and 5(b), respectively. The depth scales have been calculated with  $E_{th}$  determined from the Arrhenius plot (see Table I). The concentration of that hole trap exhibits a maximum at about 250 nm. The DLTFs peak temperature shifts in the as-grown sample from 158 to 168 K for deep-level responses close to 250 nm. This point is identical to the position of the normal interface obtained from the SIMS depth profile in Fig. 1. The total amount of level HK2 is not changed by annealing, but the spatial distribution is broadened around the normal interface, in contrast to trap HK1.

Other properties of levels HK1 and HK2 are very similar. The associated defects accumulate at the Ga(As, N)-on-GaAs interface. Their activation energies  $E_\sigma$  for capturing holes are negligible. The densities of both interfacial states are comparable and found to be about  $6 \times 10^9 \text{ cm}^{-2}$ . The two defects cannot be removed by rapid thermal annealing. As for level HK1, a further shift of the DLTFs peak to lower temperature is also detected for hole trap HK2 at about 310

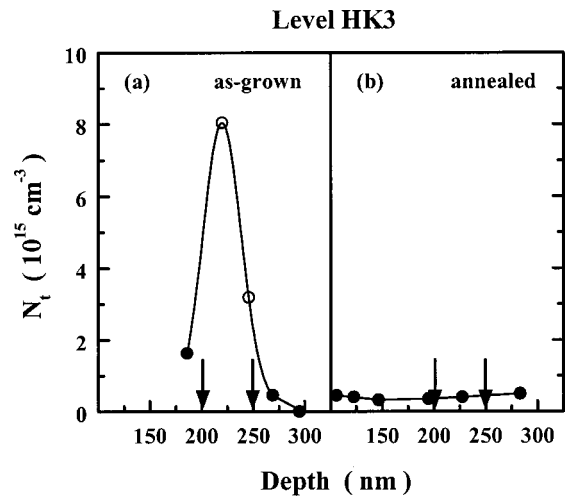


FIG. 6. Concentration vs depth profiles for hole trap HK3 derived from deep-level spectra on (a) the as-grown and (b) annealed heterostructure No. 2. The interface positions are indicated by arrows. The DLTFs peak temperatures of 190 K for Ga(As,N) and 205 K for GaAs are marked in (a) by circles and dots, respectively. For the annealed sample in (b), the exact peak temperatures could not be determined. The data in (a) are fitted by a Gaussian curve. The total amount of level HK3 in as-grown sample No. 2 is found to be about  $4 \times 10^{10} \text{ cm}^{-2}$ .

nm [see the square symbol in Fig. 5(a)]. Level HK2 originates apparently also from a defect, which is generated on the growing GaAs surface even when the rf plasma cell is operated with a closed shutter. The defect is, however, not directly related to the incorporation of nitrogen into GaAs, because the trap density decreases inside the Ga(As, N) layer.

## 3. Hole trap HK3

The concentration of hole trap HK3 is comparably low in as-grown heterostructure No. 1 (see Fig. 3). It becomes, however, dominant in other structures investigated. Figures 6(a) and 6(b) display the concentration versus depth profiles for hole trap HK3 in the as-grown and annealed sample No. 2. Whereas a giant peak is observed in the as-grown Ga(As, N) layer, the level density is strongly reduced in the annealed sample. The depth scales in Fig. 6 have been determined by using the thermal activation energy  $E_{th}$  (see Table I). It is seen from Fig. 6(a) that the transition from the higher to the lower DLTFs peak temperature occurs at about 200 nm, which is the position of the GaAs-on-Ga(As, N) interface.

The use of the thermal activation energy  $E_{th}$  instead of the true level energy  $E_t$  is therefore allowed for hole trap HK3 like for levels HK1 and HK2, i.e., the capture process is practically not thermally activated. The energy of level HK3 changes from about 0.37 to 0.35 eV by crossing the interface from GaAs to Ga(As, N). It is the same bulk defect which gives rise to the discrete levels on both sides of the heterojunction. Its concentration can reach values of  $1 \times 10^{16} \text{ cm}^{-3}$  in the Ga(As,N) layer.

## 4. Hole trap HK4

Hole trap HK4 is the other relevant defect level in all the as-grown *p*-type GaAs/Ga(As, N)/GaAs heterostructures in-

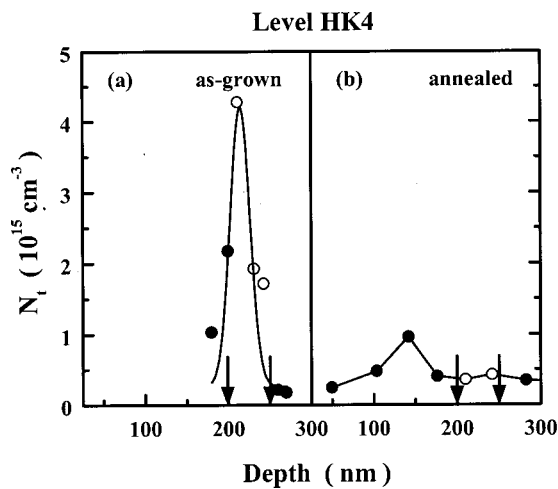


FIG. 7. Typical concentration vs depth profiles for hole trap HK4 derived from deep-level spectra on (a) the as-grown and (b) annealed heterostructure No. 1. The data have been evaluated with energy  $E_t$  of 0.45 eV. The interface positions are indicated by arrows. The DLTS peak temperatures of 250 K for Ga(As,N) and 260 K for GaAs are marked by circles and dots, respectively. The data in (a) are fitted by a Gaussian curve. The total amount of level HK4 in as-grown sample No. 1 is found to be about  $2 \times 10^{10} \text{ cm}^{-2}$ .

investigated. Figures 7(a) and 7(b) display typical concentration versus depth profiles for hole trap HK4, measured in the as-grown and annealed heterostructure No. 1, respectively. The depth profile of the as-grown structure in Fig. 7(a) shows in the Ga(As, N) layer a high trap concentration of about  $4 \times 10^{15} \text{ cm}^{-3}$ . The depth scales in Fig. 7 have been determined by assuming an energy  $E_t$  of 0.45 eV instead of the thermal activation energy  $E_{th}$  of about 0.55 eV obtained from Arrhenius plots. By using this level energy, the DLTS response at 250 K, which is due to level HK4 in Ga(As, N), could be placed between the well-known interface positions at 200 and 250 nm of sample No. 1. We have to assume therefore that the hole capture process at level HK4 is thermally activated with energy  $E_{\sigma}$  of about 0.10 eV.

As for hole trap HK3, the maximum concentration of level HK4 is found close to the GaAs-on-Ga(As, N) interface [see Fig. 7(a)]. The defect density in Ga(As, N) can be drastically reduced by RTA [see Fig. 7(b)]. The underlying defect reactions seem to be more effective in Ga(As, N) than in GaAs, since some of the HK4 traps, which moved from Ga(As, N) into GaAs, are not completely removed by annealing [see the small peak in Fig. 7(b) around 150 nm].

#### D. Deep-level identification

In order to identify hole traps HK1, HK2, HK3, HK4, and HK5 in the heterojunctions investigated, their respective thermal emission rates  $e_p$  are compared in Fig. 8 with levels, which are commonly found in *p*-type GaAs.<sup>22-26</sup> It should be noted that nitrogen-related defects give rise to electron traps.<sup>27</sup> They can be ignored therefore as origins of hole traps.

It is evident from Fig. 8 that levels HK2 and HK5 are identical to well-known hole traps A and B, which are the dominant levels in GaAs grown by liquid phase epitaxy

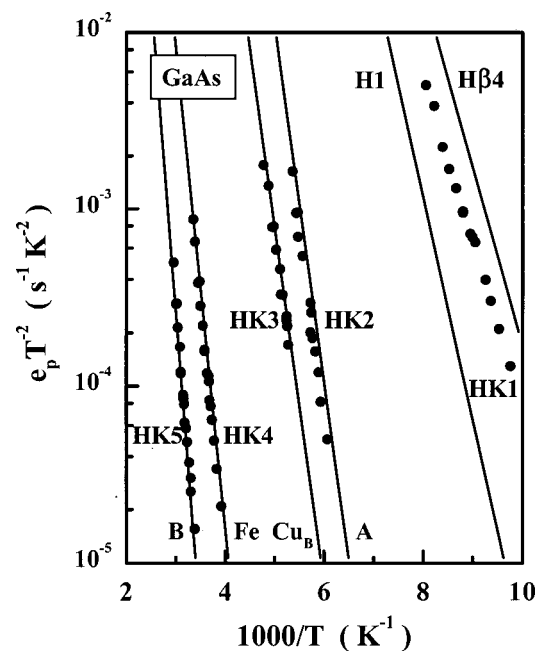


FIG. 8. Arrhenius plots for hole traps HK1, HK2, HK3, HK4, and HK5 in the GaAs layers of GaAs/Ga(As,N)/GaAs heterostructures (dots) compared with published data (lines) for the irradiation-induced hole traps, H $\beta$ 4 (Ref. 22) and H1 (Ref. 23), the two levels A and B typical of LPE-grown GaAs (Ref. 24), the Cu<sub>B</sub> level (Ref. 25), and the trap due to Fe in GaAs (Refs. 26).

(LPE).<sup>24</sup> They originate from the Ga<sub>As</sub> antisite defect (Ga atom on an As site),<sup>24,28</sup> which is an intrinsic double donor. The levels A and B correspond to the charge state changes Ga<sub>As</sub><sup>0/-</sup> and Ga<sub>As</sub><sup>-2/-</sup>, respectively. In contrast to LPE-grown GaAs, where the levels are found as bulk states, hole traps HK2 and HK5 are observed here spatially localized at the MBE-grown Ga(As, N)-on-GaAs interface (see Fig. 5) and at the surface of the GaAs top layer (see curve 1 in Fig. 3), respectively. It is a general phenomenon that Ga<sub>As</sub> antisite defects are formed during epitaxial GaAs growth near the *p*-type surface,<sup>29</sup> because the defect formation energy, which depends strongly on the position of the Fermi level,<sup>30</sup> becomes smaller at the surface.

The origin of level HK1 is not fully clear yet. This level is usually not present in MBE-grown GaAs. There are only a few papers which report on hole traps with comparable properties.<sup>22,23</sup> In Fig. 8, two Arrhenius plots are depicted (lines H1 and H $\beta$ 4), which originate from point defects in the As sublattice formed by particle irradiation.<sup>22,23</sup> It is therefore suggested that level HK1 close to the Ga(As, N)-on-GaAs interface is due to an intrinsic lattice imperfection, which is generated at the GaAs surface when the growth conditions are slightly modified by the rf plasma. The relatively small amount of this defect cannot be annealed out.

The dominant levels, HK3 and HK4, in the lower half of the band gap exhibit properties identical to those of well-known hole traps in GaAs, which are associated with Cu and Fe atoms on Ga sites, respectively (see Fig. 8).<sup>25,26,31</sup> The extrinsic origin of level HK4 is further confirmed, since, in complete agreement with the results of Ref. 26, its capture cross section for holes is found to be thermally activated with energy  $E_{\sigma}$  of about 0.10 eV (see Sec. III C4). It should

TABLE II. Identification of the hole traps in *p*-type GaAs/Ga(As,N)/GaAs heterojunctions: Correspondence between the HK levels of this study and deep levels in GaAs material known from other publications.

HK levels in this work		Hole traps in GaAs detected elsewhere		
Label	Label	$E_{th}$ (eV)	Process	Origin
HK1	H $\beta$ <sup>a</sup>	0.20	Irradiation	As sublattice <sup>a,b</sup>
	H1 <sup>b</sup>	0.25	Irradiation	
HK2	A <sup>c</sup>	0.40	LPE	Ga <sub>As</sub> <sup>0/-</sup> c,d
	HB5 <sup>c</sup>	0.40	LPE	
HK3	Cu <sub>B</sub> <sup>f</sup>	0.40	Cu diffusion	Cu <sub>Ga</sub> defect <sup>e,f</sup>
	HL4 <sup>c</sup>	0.42	Cu diffusion	
	H2 <sup>b</sup>	0.40	VPE <sup>g</sup>	
HK4	Fe <sup>h</sup>	0.54	Fe diffusion	Fe <sub>Ga</sub> defect <sup>h,i</sup>
	HB3 <sup>c</sup>	0.52	Fe doped	
	H3 <sup>b</sup>	0.51	VPE <sup>g</sup>	
HK5	B <sup>c</sup>	0.70	LPE	Ga <sub>As</sub> <sup>-2/-</sup> c,d
	HB2 <sup>c</sup>	0.71	LPE	

<sup>a</sup>Reference 22.

<sup>b</sup>Reference 23.

<sup>c</sup>Reference 24.

<sup>d</sup>Reference 28.

<sup>e</sup>Reference 32.

<sup>f</sup>Reference 25.

<sup>g</sup>Vapor-phase epitaxy.

<sup>h</sup>Reference 26.

<sup>i</sup>Reference 31.

be noted that optical and thermal energies for the Cu-related level match each other,<sup>25</sup> i.e., the thermal activation energy for the hole capture process is negligible, in accordance with our findings for hole trap HK3. Both extrinsic defects are commonly not observed in MBE-grown GaAs, nor are they after irradiation.<sup>22</sup> The predominant occurrence of these impurities in Ga(As, N) is apparently linked with operation of the rf plasma source or the nitrogen purity.

The results concerning the identification of the deep-level defects in as-grown *p*-type GaAs/Ga(As, N)/GaAs heterostructures are compiled in Table II.

#### IV. CONCLUSIONS

Intrinsic and extrinsic defects are identified in MBE-grown GaAs/Ga(As, N)/GaAs heterostructures. The intrinsic hole traps, HK1 and HK2, are directly related to the GaAs growth conditions, which are apparently modified by operation of the rf plasma cell. These intrinsic defects, which are generated close to the Ga(As, N)-on-GaAs interface, are resistant to annealing. Their concentrations at the normal interface are low, being in the  $10^9$  cm<sup>-2</sup> range.

The extrinsic midgap levels, HK3 and HK4, in the Ga(As, N) layer possess hole capture cross sections  $\sigma_p$  of about  $1 \times 10^{-14}$  and  $1 \times 10^{-15}$  cm<sup>2</sup>, respectively. From the expression  $\tau_p = 1/\sigma_p v_{th} N_t$ , the lifetime  $\tau_p$  for holes can be estimated to be lower than 1 ns in the heterostructures investigated, which is in agreement with measured photoluminescence lifetimes.<sup>33,34</sup> The degradation of the optical properties of Ga(As, N) may be therefore, at least partially, connected with the occurrence of impurity-related defect levels HK3 and HK4 at  $E_v + 0.35$  and  $+0.45$  eV, respectively.

The strong carrier deficit observed in all as-grown *p*-type GaAs/Ga(As, N)/GaAs structures is caused by deep donor-like levels.<sup>3</sup> Since the incorporation of Cu and Fe gives rise to acceptor-like levels, i.e., negatively charged (empty state)

and neutral (occupied by a hole), the carrier depletion in *p*-type Ga(As, N) cannot be explained by these impurity-related traps. Furthermore, the measured densities of traps HK3 and HK4 are about one order of magnitude lower than the carrier deficit found in the investigated heterostructures. We therefore believe that deep donor-like levels in the upper half of the band gap must be considered in order to fully understand the degradation of the electronic properties of Ga(As, N).

#### ACKNOWLEDGMENTS

The authors are very grateful for the technical assistance of H. Kostial and E. Wiebicke. The authors are indebted to H. T. Grahn and M. Wassermeier for comments and for careful reading of the manuscript. This research was partially funded by DARPA and ARO through Contract No. DAAG 55-98-1-0437.

<sup>1</sup>M. Weyers, M. Sato, and H. Ando, *Jpn. J. Appl. Phys.*, Part 2 **31**, L853 (1992).

<sup>2</sup>M. Weyers and M. Sato, *Appl. Phys. Lett.* **62**, 1396 (1993).

<sup>3</sup>P. Krispin, S. G. Spruytte, J. S. Harris, and K. H. Ploog, *J. Appl. Phys.* **88**, 4153 (2000).

<sup>4</sup>M. Kondow, K. Uomi, A. Niwa, T. Kitatani, S. Watahiki, and Y. Yazawa, *Jpn. J. Appl. Phys.*, Part 1 **35**, 1273 (1996).

<sup>5</sup>S. Sato, Y. Osawa, and T. Saitoh, *Jpn. J. Appl. Phys.*, Part 1 **36**, 2671 (1997).

<sup>6</sup>H. P. Xin and C. W. Tu, *Appl. Phys. Lett.* **72**, 2442 (1998).

<sup>7</sup>T. Miyamoto, K. Takeuchi, T. Kageyama, F. Koyama, and K. Iga, *Jpn. J. Appl. Phys.*, Part 1 **37**, 90 (1998).

<sup>8</sup>M. C. Larson, M. Kondow, T. Kitatani, K. Nakahara, K. Tamura, H. Inoue, and K. Uomi, *IEEE Photonics Technol. Lett.* **10**, 188 (1998).

<sup>9</sup>A. Wagner, C. Ellmers, F. Höhnsdorf, J. Koch, C. Agert, S. Leu, M. Hofmann, W. Stolz, and W. W. Rühle, *Appl. Phys. Lett.* **76**, 271 (2000).

<sup>10</sup>C. W. Coldren, M. C. Larson, S. G. Spruytte, and J. S. Harris, *Electron. Lett.* **36**, 951 (2000).

<sup>11</sup>S. R. Kurtz, A. A. Allerman, E. D. Jones, J. M. Gee, J. J. Banas, and B. E. Hammons, *Appl. Phys. Lett.* **74**, 729 (1999).

<sup>12</sup>S. Francoeur, G. Sivaraman, Y. Qiu, S. Nikishin, and H. Temkin, *Appl. Phys. Lett.* **72**, 1857 (1998).

<sup>13</sup>E. V. K. Rao, A. Ougazzaden, Y. Le Bellego, and M. Juhel, *Appl. Phys. Lett.* **72**, 1409 (1998).

<sup>14</sup>A. Moto, S. Tanaka, N. Ikoma, T. Tanabe, S. Takagishi, M. Takahashi, and T. Katsuyama, *Jpn. J. Appl. Phys.*, Part 1 **38**, 1015 (1999).

<sup>15</sup>G. Pozina, I. Ivanov, B. Monemar, J. V. Thordson, and T. G. Andersson, *J. Appl. Phys.* **84**, 3830 (1998).

<sup>16</sup>T. Prokofyeva, T. Sauncy, M. Seon, M. Holtz, Y. Qiu, S. Nikishin, and H. Temkin, *Appl. Phys. Lett.* **73**, 1409 (1998).

<sup>17</sup>S. G. Spruytte, C. W. Coldren, A. F. Marshall, M. C. Larson, and J. S. Harris, *Mater. Res. Soc. Symp. Proc.* **595**, W8.4.1 (2000).

<sup>18</sup>P. Blood and J. W. Orton, *The Electrical Characterization of Semiconductors: Majority Carriers and Electron States* (Academic, London, 1992).

<sup>19</sup>S. Weiss and R. Kassing, *Solid-State Electron.* **31**, 1733 (1988).

<sup>20</sup>D. V. Lang, *J. Appl. Phys.* **45**, 3023 (1974).

<sup>21</sup>J. Bourgoin and M. Lannoo, *Point Defects in Semiconductors II: Experimental Aspects* (Springer, Berlin, 1983), p. 167.

<sup>22</sup>F. D. Auret, S. A. Goodman, W. E. Meyer, R. M. Erasmus, and G. Myburg, *Jpn. J. Appl. Phys.*, Part 2 **32**, L974 (1993).

<sup>23</sup>S. Loualiche, A. Nouailhat, G. Guillot, M. Gavand, A. Laugier, and J. C. Bourgoin, *J. Appl. Phys.* **53**, 8691 (1982).

<sup>24</sup>Z.-G. Wang, L.-A. Ledebø, and H. G. Grimmeiss, *J. Phys. C* **17**, 259 (1984).

<sup>25</sup>N. Kullendorff, L. Jansson, and L.-Å. Ledebø, *J. Appl. Phys.* **54**, 3203 (1983).

<sup>26</sup>M. Kleverman, P. Omling, L.-Å. Ledebø, and H. G. Grimmeiss, *J. Appl. Phys.* **54**, 814 (1983).

- <sup>27</sup>D. J. Wolford, J. A. Bradley, K. Fry, and J. Thompson, in *Proceedings of the 17th International Conference on the Physics of Semiconductors*, edited by J. D. Chadi and W. A. Harrison (Springer, New York, 1985), p. 627.
- <sup>28</sup>P. Krispin, *J. Appl. Phys.* **65**, 3470 (1989).
- <sup>29</sup>P. Krispin, M. Asghar, H. Kostial, and R. Hey, *Physica B* **273–274**, 693 (1999).
- <sup>30</sup>S. B. Zhang and J. E. Northrup, *Phys. Rev. Lett.* **67**, 2339 (1991).
- <sup>31</sup>S. G. Bishop, in *Deep Centers In Semiconductors*, edited by S. T. Pantelides (Gordon and Breach, New York, 1986).
- <sup>32</sup>A. Mitonneau, G. M. Martin, and A. Mircea, *Electron. Lett.* **13**, 666 (1977).
- <sup>33</sup>I. A. Buyanova, W. M. Chen, G. Pozina, J. P. Bergman, B. Monemar, H. P. Xin, and C. W. Tu, *Appl. Phys. Lett.* **75**, 501 (1999).
- <sup>34</sup>R. A. Mair, J. Y. Lin, H. X. Jiang, E. D. Jones, A. A. Allerman, and S. R. Kurtz, *Appl. Phys. Lett.* **76**, 188 (2000).